Angiogenesis (2012) 15:349–360
DOI 10.1007/s10456-012-9265-1

ORIGINAL PAPER

$P2Y_4$ nucleotide receptor: a novel actor in post-natal cardiac development

Michael Horckmans · Bernard Robaye · Elvira Léon-Gómez · Nicolas Lantz · Philippe Unger · Frédérique Dol-Gleizes · Sophie Clouet · Dorothée Cammarata · Paul Schaeffer · Pierre Savi · Christian Gachet · Jean-Luc Balligand · Chantal Dessy · Jean-Marie Boeynaems · Didier Communi

Received: 27 October 2011 / Accepted: 10 March 2012 / Published online: 22 March 2012

Abstract Communication between endothelial cells and cardiomyocytes is critical for cardiac development and regeneration. However the mechanisms involved in these endothelial-cardiomyocyte interactions remain poorly understood. Nucleotides are released within the heart, especially under ischemia or pressure overload. The function of P2Y nucleotide receptors in cardiac development has never been investigated. Here we show that adult $P2Y_4$-null mice display microcardia. $P2Y_4$ nucleotide receptor is expressed in cardiac endothelial cells but not in cardiomyocytes. Loss of $P2Y_4$ in cardiac endothelial cells strongly inhibits their growth, migration and PDGF-B secretion in response to UTP. Proliferation of microvessels and cardiomyocytes is reduced in $P2Y_4$-null hearts early after birth, resulting in reduced heart growth. Our study uncovers mouse $P2Y_4$ receptor as an essential regulator of cardiac endothelial cell function, and illustrates the involvement of endothelial-cardiomyocyte interactions in post-natal heart development. We also detected $P2Y_4$ expression in human cardiac microvessels. $P2Y_4$ receptor could constitute a therapeutic target to regulate cardiac remodelling and post-ischemic revascularisation.

Keywords Heart development · Angiogenesis · Nucleotides · Endothelial cells · P2Y receptors

M. Horckmans · S. Clouet · J.-M. Boeynaems · D. Communi (✉)
Institute of Interdisciplinary Research, IRIBHM, Université Libre de Bruxelles, Building C (5th floor), Campus Erasme, 808 Route de Lennik, 1070 Brussels, Belgium
e-mail: communid@ulb.ac.be

B. Robaye · D. Cammarata
Institute of Interdisciplinary Research, IRIBHM, Université Libre de Bruxelles, 6041 Gosselies, Belgium

E. Léon-Gómez · J.-L. Balligand · C. Dessy
Unit of Pharmacology and Therapeutics, Université catholique de Louvain, UCL-FATH 5349, 1200 Brussels, Belgium

N. Lantz · C. Gachet
Department Biologie et pharmacologie des plaquettes sanguines: hémostase, thrombose, transfusion, UMR_S949 INSERM-Université de Strasbourg, Etablissement Français du Sang-Alsace, 67081 Strasbourg, France

P. Unger
Department of Cardiology, Erasme Hospital, Université Libre de Bruxelles, 1070 Brussels, Belgium

F. Dol-Gleizes · P. Schaeffer · P. Savi
Département Thrombose and Angiogenèse, Service de Pharmacologie, Sanofi-Aventis, 31300 Toulouse, France

J.-M. Boeynaems
Department of Laboratory Medicine, Erasme Hospital, Université Libre de Bruxelles, 1070 Brussels, Belgium

Introduction

Despite their importance in cardiac development, endothelial-cardiomyocyte interactions remain poorly understood [1]. Cardiac endothelial cells and cardiomyocytes are an important source of extracellular nucleotides within the heart, especially under ischemia [2] or pressure overload [3]. Extracellular nucleotides can produce trophic effects in many cell types acting at both ionotropic P2X receptors and G-protein coupled P2Y receptors. Dynamic expression of P2Y receptors in mammalian development has been previously studied [4] but their function in cardiac development has never been investigated.

In this study, we investigated the potential role of one of them, the $P2Y_4$ receptor, in heart growth and function. The human $P2Y_4$ receptor has been described as a UTP receptor

coupled to the phosphoinositide/Ca^{2+} pathway and encoded by a gene located on chromosome X [5]. Recombinant rat and mouse orthologs of human $P2Y_4$ receptor are activated by UTP and ATP [6–8], as described for the ubiquitously expressed mouse $P2Y_2$ receptor [9].

The $P2Y_4$ receptor displays a very restricted tissue distribution. So far a loss of nucleotide-induced epithelial chloride and potassium transport in the jejunum and colon is the only defect observed in $P2Y_4$ knockout mice [10–12]. Interestingly $P2Y_2$ and $P2Y_4$ receptors were abundantly detected in the rat developing heart [4]. Extracellular nucleotides are involved in protection of rat cardiomyocytes from hypoxic stress through activation of $P2Y_2$ nucleotide receptors [13]. UTP administration to rats reduced infarct size and enhanced myocardial function [14].

In this paper, we demonstrate that loss of mouse $P2Y_4$ receptor is associated with angiogenic defects and a microcardia phenotype.

Materials and methods

Ethics statement

All animal work has been conducted according to relevant national and international guidelines and approved by the ethics committee of the Free University of Brussels.

Materials

$P2Y_4^{0/+}$ and $P2Y_4^{0/-}$ CD1/C57Bl6 male mice used were generated in our institute as described [10]. Human right atrial and left ventricular tissue specimens were obtained from patients undergoing cardiac surgery. All tissue collection procedures were approved by the local Ethics Committee. Anti-$P2Y_4$ antibody was purchased from Alomone Labs (Jerusalem, Israël). Anti-CD31 (PECAM-1) and the rat isotype IgG2 antibodies were purchased from BD Biosciences (Le Pont-de-Claix, France). Anti-troponin, anti-EdU and anti-BrdU were from Abcam (Cambridge, UK). The secondary antibodies were from Jackson ImmunoResearch (Suffolk, UK). Collagenase B and DNAse I grade II were purchased from Roche Diagnostics (Vilvorde, Belgium). Calcein was obtained from Invitrogen (Merelbeke, Belgium). UTP, ATP, VEGF, FGF-2, sphingosine 1-phosphate (S1P), Drabkin kit, mouse IgG2a, trypsin were purchased from Sigma Aldrich (Saint Quentin Fallavier, France). Matrigel and Matrisperse were obtained from BD Biosciences (Le Pont-de-Claix, France). Paraformaldehyde and paraffin were from Merck Eurolab (Strasbourg, France). Serum, biotinylated antibody and Novared kit were obtained from Coger (Paris, France).

Echocardiography of $P2Y_4^{0/+}$ and $P2Y_4^{0/-}$ mice

Twelve weeks old mice were anesthetised using ketamine (150 mg/kg) for echocardiographic experiments. Cardiac dimensions were derived from the mean of five measurements. Analysis of the echocardiographic data was done blinded to the type of strain.

In situ RNA hybridization

In situ RNA hybridization using digoxigenin-labelled RNA probes on fixed heart cryosections was performed as described [15]. Immunodetection was performed using standard methods. All stainings were performed on two hearts extracted from $P2Y_4^{0/+}$ mice.

Isolation of primary mouse $P2Y_4^{0/+}$ and $P2Y_4^{0/-}$ endothelial cells (ECs)

ECs were isolated from mouse hearts and lungs as previously described [16]. ECs have been collected from 6 to 8 weeks mice, after a collagenase B (2 mg/mL), DNaseI (0.5 mg/mL) treatment and a Percoll gradient. ECs were cultured on collagen-coated dishes using EBM medium with 2 % FBS, 10 ng/mL EGF, 1 μg/mL hydrocortisone and 12 μg/mL bovine brain extract and 100 μg/ml heparin. The purity of the cultures was checked using CD31 staining.

Isolation of mouse $P2Y_4^{0/+}$ and $P2Y_4^{0/-}$ cardiomyocytes

The protocol was based on the procedure previously reported by Alvarez et al. [17]. Briefly, hearts were excised from 10 days old or 12 weeks old mice. Left ventricles were quickly removed, cut and digested by collagenase B (2 ng/mL). Cells collected by gravitational and centrifugational sedimentation were pooled and resuspended in HBSS 0.1 % BSA.

Quantitative RT-PCR experiments

Total RNAs were extracted using TRIzol reagent (Life Technologies, Groningen, Netherlands) and RNeasy kit (Qiagen, Hilden, Germany). RNA was reverse transcribed using random hexamers and Superscript II Reverse Transcriptase. RT-PCR experiments were run on a 7500 Fast Real Time PCR System (Applied Biosystems). Mean ± SD of ratios was obtained using qBase software. Each assay was performed in duplicate for at least two independent preparations of ECs. CD31 and troponin were used as positive controls for respectively ECs and cardiomyocytes. PCR data were normalized to RPL13 and HPRT. For PCR data, obtained from human atrium, ventricle and

microvessels, were normalized to B2M and 18S. For PDGF-B quantification, heart ECs were stimulated by UTP (100 μmol/L) for 6 h. Total RNAs were isolated as described above and data were normalized to RPL13 and HPRT.

Calcium measurements

Calcium levels were measured at RT with the fura-2 Ca^{2+}-binding dyes. Cardiomyocytes were labelled during 30 min with fura-2/AM (2.5 μg/ml) (Molecular Probes, Leiden, The Netherlands) and placed at 37 °C. For fura-2 assays, fluorescence was determined in an LS-50B fluorometer (Perkin Elmer, Überlingen, Germany). All measurements were carried out at room temperature. The fluorescence ratio (F_{360}/F_{380}) reflects the intracellular calcium concentration.

Migration and growth assays of $P2Y_4^{0/+}$ and $P2Y_4^{0/-}$ ECs

Chemotaxis of primary ECs was assayed in a multiwell chamber as described previously [18]. Briefly ECs were allowed to migrate through a Polyvinylpyrrolidone coated filter (8 μm hole size) in response to UTP during 4 h at 37 °C. The number of migrated cells was counted with an image analyzer (ImageJ Program; NIH). For the growth assays, 4×10^4 ECs were placed in EBM medium (0.1 % FBS) during 24 h. The cells were then stimulated during 72 h by UTP 100 μmol/L or VEGF 100 ng/ml and counted manually.

PDGF-B elisa

Supernatants of cardiac ECs or sera of $P2Y_4^{0/+}$ and $P2Y_4^{0/-}$ mice were collected and PDGF-BB levels were measured by enzyme-linked immunosorbent assay using the Quantikine kit from R&D Systems (Abingdon, GB).

Immunohistochemistry experiments

After cervical dislocation, hearts were harvested, weighed and frozen directly in OCT compound (VWR Scientific). Heart sections (7 μm) were fixed with methanol and stained with hematoxylin/eosin (HE), DAPI and antibodies against $P2Y_4$, CD31 or troponin. Microvessel and cardiomyocyte density were quantified in complete transversal cross-sections by examining 15 fields per section covering at least 40 % of each tested heart, at 20× magnification, in a blinded fashion. For BrdU labelling, 10 days old mice were injected intraperitoneally with a single pulse (50 μg/g body weight) of BrdU, 24 h before sacrifice. To quantify the proliferation of microvessels, the number of double labeled CD31/BrdU vessels was normalized to total CD31 positive vessels.

To quantify cardiomyocyte size, microscope lighting, focus, and field selection were optimized for distinction of cell boundaries. Fields were chosen to increase the probability of cardiomyocytes being visualized in appropriate cross-section and not tangentially. Cardiomyocytes were outlined manually and cardiomyocytes size was measured using Image J software.

Quantification of endothelial and cardiomyocyte proliferation by flow cytometry experiments

Five days old $P2Y_4^{0/+}$ and $P2Y_4^{0/-}$ mice were injected intraperitoneally with a single pulse (50 μg/g body weight) of EdU, 24 h before sacrifice. The number of double labeled troponin/Edu and CD31/EdU cells was measured by flow cytometry using cell suspensions obtained from whole hearts after collagenase B (2 mg/mL) treatment.

Matrigel experiments

Matrigel with 1.4 μg/mL VEGF, 8 μg/mL FGF-2 and 500 nmol/L S1P and 116 μg/mL BSA Fatty Acid Free was subcutaneously injected in the median line of the abdomen during 14 days. Paraffin slides (5 μm) were colored with HE and the total area occupied by colored cells was quantified with the image analysis software Metamorph (Universal Imaging Corp., West Chester, US). The cellularities were expressed in pixels and represented the ratio between the area of colored cells and the total area of the selected field. The data displayed are the mean of at least three different slides covering the totality of the matrigel.

Murine air pouch granuloma

This model of inflammatory angiogenesis was performed essentially as described [19]. Five-milliliter air pouches were raised on the dorsal surface of female mice (6–8 weeks old). After 4 h, 0.5 mL of 0.1 % v/v croton oil in Freund's complete adjuvant (Sigma) was injected into the pouch. 8 days later, a vascular cast was made by intravenous injection of 1 mL of a solution of 5 % carmine red/10 % gelatin. The granuloma tissue was removed, dried, weighed and digested. Carmine content was determined against a carmine standard curve read at 490 nm.

Statistics

Data are expressed as mean ± SEM for in vitro and vivo studies. Endpoint comparisons with 2 groups were performed

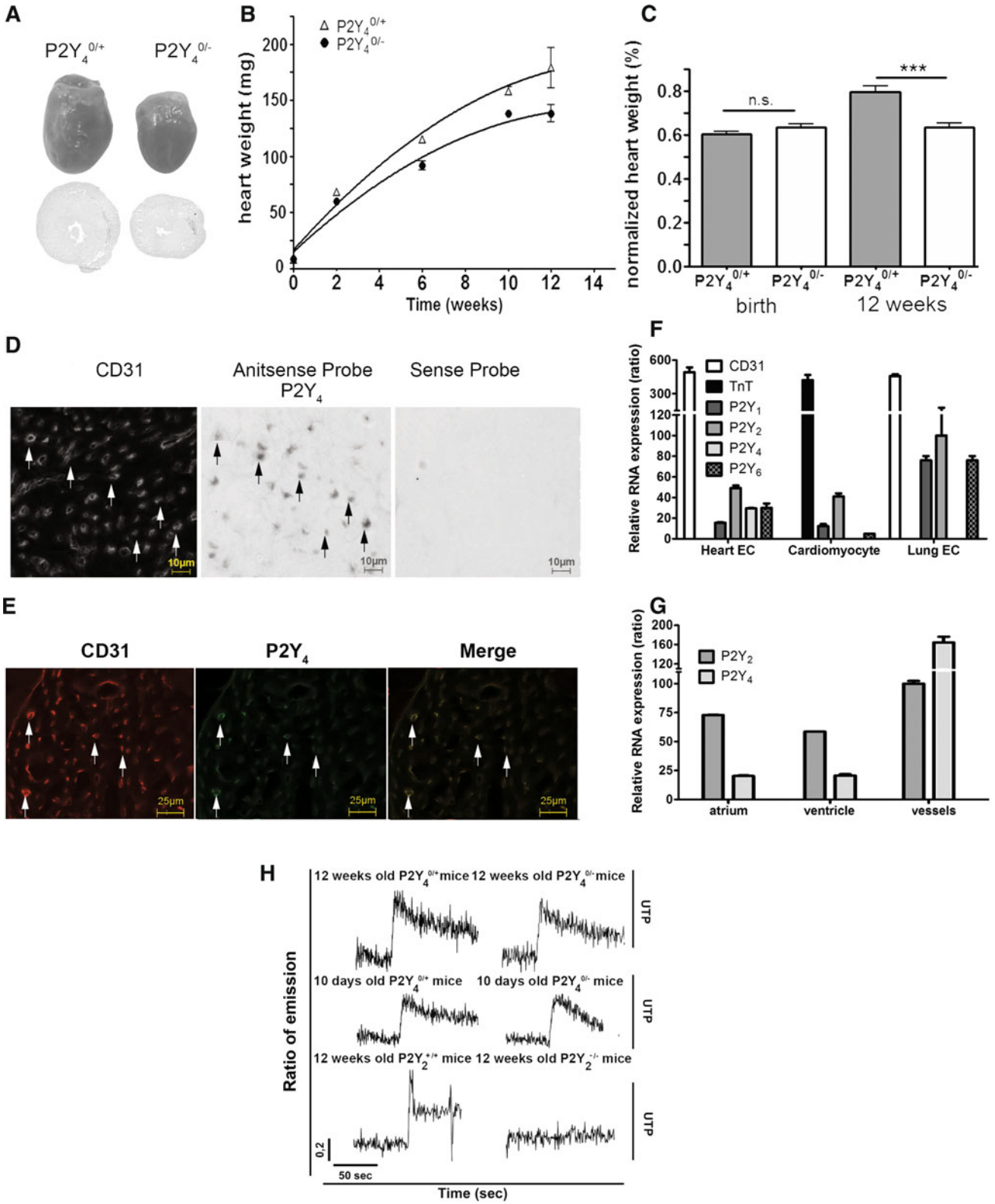

using an unpaired 2-tailed Student's *t* test (Prism Software, version5; GraphPad, CA). For parallel repeated-measures studies, 2-way ANOVA was used with Bonferroni post hoc evaluations to determine the significance for individual time points (Prism Software; GraphPad). For all studies, p value was considered as, $*p < 0.05$; $**p < 0.01$; $***p < 0.001$.

◀ **Fig. 1** Microcardia phenotype of the $P2Y_4$-null mice. **a** Typical hearts of 12 weeks old $P2Y_4^{0/+}$ and $P2Y_4^{0/-}$ mice. Frozen sections (7 μm) of whole hearts of $P2Y_4^{0/+}$ mice and $P2Y_4^{0/-}$ mice were stained with hematoxylin-eosin. Images were taken at the same magnification of ×2.5. **b** Post-natal heart weight of 0, 2, 6, 10 and 12 weeks-old $P2Y_4^{0/+}$ and $P2Y_4^{0/-}$ mice. Heart weight of male mice from newborn to adult (12 weeks) is plotted versus age. Curves were fit using nonlinear regression. Each data point represent the mean ± SEM of five mice. **c** Normalized heart weight of newborn and 12 weeks-old $P2Y_4^{0/+}$ and $P2Y_4^{0/-}$ mice. Heart weight was normalized according to mouse body weight for newborn and 12 weeks old $P2Y_4^{0/+}$ and $P2Y_4^{0/-}$ mice (means ± SEM of 8 mice per genotype). **d** Expression of $P2Y_4$ mRNA in 10 days old $P2Y_4^{0/+}$ heart. The expression of $P2Y_4$ mRNA is demonstrated by in situ hybridization with antisense probe against a fragment of $P2Y_4$, control hybridization with the corresponding sense probe and CD31 labeling of the adjoining section (×40 magnification). Some $CD31^+$-microvessels that are positive for $P2Y_4$ expression are indicated by white arrows. **e** Immunodetection of $P2Y_4$ expression in adult $P2Y_4^{0/+}$ heart. Microscopic analysis at ×20 magnification showing co-localization of CD31 (*red*) and $P2Y_4$ (*green*) in adult $P2Y_4^{0/+}$ and $P2Y_4^{0/-}$ mice. *White arrows* indicate examples of microvessels and vessels identified by a double labelling CD31/$P2Y_4$. **f** Expression of $P2Y_1$, $P2Y_2$ and $P2Y_4$ and $P2Y_6$ mRNAs in mouse cardiac endothelial cells, lung endothelial cells and cardiomyocytes. Quantitative RT-PCR experiments were performed using specific primers of mouse $P2Y_2$ and $P2Y_4$ receptors and cDNA obtained after reverse transcription of three independent RNA preparation extracted from heart and lung endothelial cells and cardiomyocytes (CM). CD31 and troponin were used as positive controls for endothelial cells and cardiomyocytes, respectively. PCR data were normalized for each gene to RPL13 and HPRT housekeeping genes. The high expression of $P2Y_2$ in the lung ECs was defined as 100 %. **g** Expression of $P2Y_2$ and $P2Y_4$ mRNAs in human heart. Quantitative RT-PCR experiments were performed using specific primers of human $P2Y_2$ and $P2Y_4$ receptors and cDNA obtained after reverse transcription of RNA extracted from human atrium, ventricle and microvessels (vessels). PCR data were normalized for each gene to B2M and 18S housekeeping genes. The expression of $P2Y_2$ in microvessels was defined as 100 %. **h** Calcium response to UTP in $P2Y_4^{0/+}$, $P2Y_4^{0/-}$, $P2Y_2^{0/+}$ and $P2Y_2^{0/-}$ cardiomyocytes. Effect of UTP (100 μmol/L) on intracellular calcium mobilization was measured in freshly isolated fura-2-loaded cardiomyocytes from adult and 10 days old mice. The ratio of emission represents the ratio between 340 and 380 nm. These data are representative of three independent experiments. (Color figure online)

Results

Microcardia phenotype of the $P2Y_4$-deficient mice

We observed that $P2Y_4$-deficient ($P2Y_4^{0/-}$) adult mice displayed a reduced heart weight compared to $P2Y_4^{0/+}$ mice (Fig. 1a), whereas the weight of other organs (lung, spleen, kidney, liver) was unchanged (data not shown). Heart wet weight of $P2Y_4^{0/+}$ and $P2Y_4^{0/-}$ mice was then compared at different ages (Fig. 1b) and was normalized to the body weight (Fig. 1c). No significant difference was observed at birth, whereas at 12 weeks the weight of $P2Y_4^{0/+}$ and $P2Y_4^{0/-}$ hearts were 173.9 ± 7.8 mg and 138.6 ± 3.3 mg respectively (means ± SEM; $***p < 0.001$; N = 13), which corresponds to a heart weight reduction of 20 % (Fig. 1c). The microcardia phenotype has been also observed by measuring the heart dry weight of male and female $P2Y_4$-deficient mice (data not shown).

Table 1 Echocardiographic assessment of $P2Y_4^{0/+}$ and $P2Y_4^{0/-}$ mice

Parameters	$P2Y_4^{0/+}$	$P2Y_4^{0/-}$	*p* values
Septal wall D (mm)	1.04 ± 0.03	0.89 ± 0.03	<0.01**
Left ventricle ED (mm)	2.99 ± 0.12	2.89 ± 0.10	NS
Posterior wall D (mm)	0.86 ± 0.03	0.75 ± 0.04	<0.05*
Septal wall S (mm)	1.63 ± 0.03	1.53 ± 0.04	<0.05*
Left ventricle ES (mm)	1.52 ± 0.07	1.36 ± 0.07	NS
Posterior wall S (mm)	1.45 ± 0.04	1.34 ± 0.03	<0.05*
Left ventricle mass (g)	0.096 ± 0.008	0.075 ± 0.005	<0.05*
Relative wall thickness	0.64 ± 0.02	0.58 ± 0.03	NS
Ejection fraction (%)	59 ± 7	63 ± 7	NS
LV cardiac output (mL/min)	16.62 ± 0.98	18.9 ± 1.32	NS
LV fractional shortening (%)	57.41 ± 1.9	59.1 ± 1.7	NS
Heart rate (bpm)	664.8 ± 11.4	651.9 ± 14.0	NS

Twelve weeks old $P2Y_4^{0/+}$ and $P2Y_4^{0/-}$ sedated mice (N = 11) were used for echocardiographic measurements (*D* diastolic; *S* systolic; *ED* end-diastolic; *ES* end-systolic). Ejection fraction = LVED volume − LVES volume/LVED volume × 100; LV cardiac output = (LVED volume − LVES volume) × HR/1,000; LV fractional shortening = LVD − LVS/LVD × 100

An echocardiographic assessment was then performed to evaluate septal wall and posterior wall thickness, and left ventricular systolic and diastolic dimensions (Table 1). We observed that several measured parameters were reduced in $P2Y_4^{0/-}$ mice. In particular diastolic septal and posterior wall thickness and left ventricle mass were significantly lower in $P2Y_4^{0/-}$ mice as compared to $P2Y_4^{0/+}$ mice (Table 1; N = 11). The ejection fraction, cardiac output, fractional shortening and heart rate, measured during these experiments after sedation with 150 mg/kg ketamine were not significantly different between $P2Y_4^{0/+}$ and $P2Y_4^{0/-}$ mice (Table 1).

P2Y expression in mouse and human hearts

We studied the expression of $P2Y_4$ receptor in mouse and human hearts (Fig. 1). In situ hybridization experiments revealed $P2Y_4$ expression in microvessels, but not in cardiomyocytes of 10 days old $P2Y_4^{0/+}$ mice (Fig. 1d). Immunohistochemistry provided similar results (Fig. 1e). Quantitative RT-PCR experiments were realized using specific primers of $P2Y_1$, $P2Y_2$, $P2Y_4$, $P2Y_6$, CD31 and troponin and cDNAs from mouse primary heart ECs, lung ECs or cardiomyocytes. As expected, CD31 and troponin were only detected respectively in primary ECs and cardiomyocytes. RT-PCR data revealed $P2Y_4$ expression in primary cardiac ECs but not in lung primary ECs or cardiomyocytes, whereas $P2Y_1$, $P2Y_2$ and $P2Y_6$ expression was detected in heart ECs,

in cardiomyocytes and more strongly in lung ECs (Fig. 1f). We have also identified a significant $P2Y_2$ expression and a weaker $P2Y_4$ expression in human atrium and ventricle (Fig. 1g). A sufficient number of microvessels were then isolated from human hearts to perform PCR experiments. Both $P2Y_2$ and $P2Y_4$ mRNAs were detected in human cardiac microvessels (Fig. 1g). Mouse cardiomyocytes were isolated from hearts of 10 days old and adult $P2Y_4^{0/+}$ and $P2Y_4^{0/-}$ mice in order to perform calcium measurements. UTP calcium responses were unaffected in $P2Y_4$-null cardiomyocytes from 10 days old and adult mice (Fig. 1h). UTP calcium response was abolished in $P2Y_2$-deficient cardiomyocytes isolated from adult mice (Fig. 1h). No microcardia phenotype was observed in $P2Y_2$-deficient mice (data not shown).

Involvement of $P2Y_4$ receptor in major functions of cardiac ECs

Functional expression of $P2Y_4$ receptor was then investigated in mouse primary ECs isolated from $P2Y_4^{0/+}$ hearts by collagenase digestion followed by a percoll gradient. Lung ECs

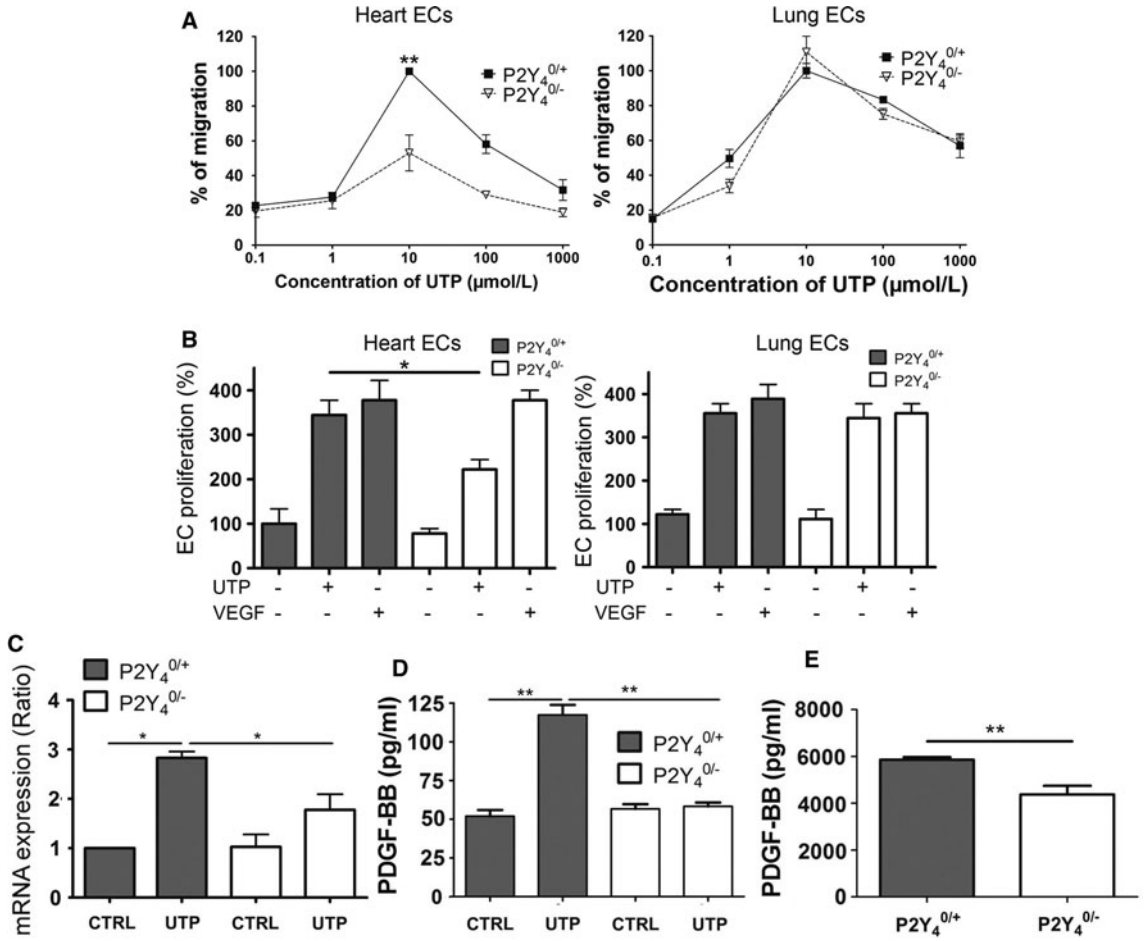

Fig. 2 Defective functions of $P2Y_4$-null cardiac endothelial cells. **a** Migration defect of primary $P2Y_4$-null cardiac endothelial cells in response to UTP. Migration of 4×10^4 primary $P2Y_4^{0/+}$ and $P2Y_4^{0/-}$ ECs isolated from heart or lungs was assayed in a multiwell chamber. Cells on filter were labelled with Hoechst and counted with an image analyzer (ImageJ Program; NIH). The data are mean ± SEM of three independent experiments. **b** Impaired proliferation of primary $P2Y_4$-null cardiac endothelial cells in response to UTP. 4×10^4 endothelial cells were stimulated in 0.1 % FBS during 72 h by UTP 100 µmol/L or VEGF 100 ng/ml and counted manually. The data are mean ± SEM of three independent experiments. **c** Impaired PDGF-B regulation in primary $P2Y_4$-null cardiac endothelial cells in response to UTP. Quantitative RT-PCR data were obtained for PDGF-B in cardiac ECs in response to UTP 100 µmol/L. Two control genes (RPL13 and HPRT) were selected after analysis using Genorm program. Normalized ratios were obtained for PDGF-B at 6 h for two independent preparation of ECs isolated from $P2Y_4^{0/+}$ and $P2Y_4^{0/-}$ hearts (mean ± SEM) using SYBR Green technology. **d** Impaired PDGF-BB release by $P2Y_4^{0/-}$ endothelial cells in response to UTP. ECs were stimulated by UTP (100 µmol/L) for 24 h. Supernatants of treated ECs were collected for ELISA measurements of PDGF-B (PDGF-BB Quantikine from R&D Systems). Results are expressed as picograms/ml and represent the mean ± SEM of two independent experiments. E. Reduction of PDGF-BB serum level in $P2Y_4$-null mice. Sera of $P2Y_4^{0/+}$ and $P2Y_4^{0/-}$ mice were collected for ELISA measurements of PDGF-B (PDGF-BB Quantikine from R&D Systems). Results are expressed as picograms/ml and represent the mean ± SEM of 8 mice

were used as a negative control of $P2Y_4$ expression in further experiments. Migration assays were performed using 4×10^4 primary ECs (Fig. 2a). The maximal effect of UTP on migration of primary ECs was observed at 10 µmol/L and was significantly decreased in $P2Y_4$-null cardiac ECs, but not in $P2Y_4$-null lung ECs (Fig. 2a). In a similar way, UTP-mediated EC proliferation was significantly reduced in $P2Y_4^{0/-}$ cardiac ECs compared to $P2Y_4^{0/+}$ cardiac ECs, whereas the VEGF effect on these cells was maintained (Fig. 2b).

Cardiac ECs are known to secrete factors such as PDGF-B and neuregulin which modulate cardiomyocyte development. Quantitative RT-PCR and ELISA experiments were performed using cardiac ECs and revealed that UTP was able to up-regulate PDGF-B expression in $P2Y_4^{0/+}$ cardiac ECs (Fig. 2c, d). No UTP effect was observed on neuregulin expression in the same cell preparations (data not shown). UTP-induced PDGF-B up-regulation was significantly inhibited in $P2Y_4^{0/-}$ cardiac ECs compared to $P2Y_4^{0/+}$ cardiac ECs (Fig. 2c, d). Interestingly serum levels of PDGF-B were significantly reduced in $P2Y_4^{0/-}$ mice (Fig. 2e).

Microvessel and cardiomyocyte proliferation defect in $P2Y_4$-deficient hearts

We analysed the density and proliferation of microvessels and cardiomyocytes in 5 days old mice by CD31 and troponin staining of heart slides (Fig. 3a) and by flow cytometry analysis (Fig. 3b). Hearts stained without primary antibodies were used as a negative control (data not shown). The number of CD31 positive microvessels was reduced in 5 days old $P2Y_4^{0/-}$ mice (45 ± 9 % of reduction; $^{**}p < 0.01$; $N = 9$) compared to 5 days old $P2Y_4^{0/+}$ mice (Fig. 3a). Cardiomyocyte density and size were not significantly affected in 5 days old $P2Y_4^{0/-}$ mice compared to $P2Y_4^{0/+}$ mice (Fig. 3a). We observed that both CD31 and troponin positive cell proliferation was significantly decreased in $P2Y_4^{0/-}$ hearts compared to $P2Y_4^{0/+}$ hearts of EdU-injected 5 days old mice (Fig. 3b). Effectively, flow cytometry data revealed a reduction of 24 ± 2 % of troponin/EdU cells ($^{***}p < 0.01$; $N = 9$) and a reduction of 22 ± 2 % of CD31/EdU positive cells ($^{***}p < 0.01$; $N = 9$) in total cell preparations from whole hearts of 5 days old $P2Y_4^{0/-}$ mice compared to 5 days old $P2Y_4^{0/+}$ mice (Fig. 3b). Apoptosis was also evaluated by the quantification of cells positive for active caspase-3 but no significant difference was observed between hearts of 5 days old $P2Y_4^{0/+}$ and $P2Y_4^{0/-}$ mice (Fig. 3c).

Immunohistochemical analysis has also been performed in 10 days old $P2Y_4^{0/-}$ and $P2Y_4^{0/+}$ mice (Fig. 3d). The number of CD31 positive microvessels was reduced in 10 days old $P2Y_4^{0/-}$ mice (20 ± 5 % of reduction; $^{**}p < 0.01$; $N = 10$) compared to 10 days-old $P2Y_4^{0/+}$ mice (Fig. 3d). The number of BrdU/CD31 double positive microvessels, normalized to the total number of vessels, was significantly reduced by 26.9 ± 9.0 % in $P2Y_4^{0/-}$ hearts compared to $P2Y_4^{0/+}$ hearts ($^{**}p < 0.01$; $N = 10$) (Fig. 3d). Cardiomyocyte density was reduced in 10 days old $P2Y_4^{0/-}$ mice compared to $P2Y_4^{0/+}$ mice (Fig. 3d). We also observed that cardiomyocyte size was significantly increased in $P2Y_4^{0/-}$ hearts compared to $P2Y_4^{0/+}$ hearts (Fig. 3d).

Microvessel and cardiomyocyte densities were also quantified in $P2Y_4^{0/+}$ and $P2Y_4^{0/-}$ adult hearts (Fig. 3e). We observed that microvessel density was reduced by 20.4 ± 2.9 % in $P2Y_4^{0/-}$ adult hearts as compared to $P2Y_4^{0/+}$ adult hearts ($^{***}p < 0.001$; $N = 8$) (Fig. 3e). The density of cardiomyocytes was reduced in adult $P2Y_4^{0/-}$ compared to adult $P2Y_4^{0/+}$ hearts (19.3 ± 6.4 % of reduction; $^{**}p < 0.01$; $N = 8$) (Fig. 3e).

$P2Y_4$-deficient mice display an angiogenic defect in matrigel and air pouch in vivo models

The role of $P2Y_4$ receptor in angiogenesis was also evaluated using in vivo models involving the proliferation of microvascular ECs. Subcutaneous injection of matrigel or croton oil in Freund's complete adjuvant was performed in $P2Y_4^{0/+}$ and $P2Y_4^{0/-}$ mice (Fig. 4). Matrigel plugs were collected 14 days after matrigel injection under the abdominal skin and were subjected to histological analysis. Haematoxylin-eosin coloration revealed that in wild-type $P2Y_4^{0/+}$ mice, cellular infiltration was detected in the periphery and the center of the matrigel, whereas in $P2Y_4^{0/-}$ mice, large parts of the matrigel were not infiltrated by cells leading to its fragilization (Fig. 4a). Total areas occupied by colored cells have been quantified to allow the comparison of the cell density between $P2Y_4^{0/+}$ and $P2Y_4^{0/-}$ mice (Fig. 4a, right panel). Cellular infiltration was similar at the periphery, but a significant difference was observed in the center of the matrigel plugs (Fig. 4a). Endothelial cells were detected at the periphery and the center of the matrigel plugs in $P2Y_4^{0/+}$ mice where as strong reduction of CD31-positive cells were observed in their center in $P2Y_4^{0/-}$ mice (Fig. 4a).

In another model, air pouches were raised on the dorsal surface of $P2Y_4^{0/+}$ and $P2Y_4^{0/-}$ mice and injected with croton oil in Freund's complete adjuvant. Eight days later, animals were anesthetized and a vascular cast was made by intravenous injection of carmine red. The granuloma tissue was then removed to determine the granuloma dry weight and dye content (Fig. 4b). A significant reduction of dry granuloma weight was observed in $P2Y_4^{0/-}$ mice compared to $P2Y_4^{0/+}$ mice: 191.4 ± 5.5 mg versus 157.0 ± 8.1 mg respectively in $P2Y_4^{0/+}$ and $P2Y_4^{0/-}$ mice (mean ± SEM; $N = 10$; $^{**}p < 0.01$) which represents a reduction of 18 % (Fig. 4b; left panel). A comparable reduction of dye content was observed: 0.91 ± 0.06 mg in $P2Y_4^{0/+}$ mice versus 0.71 ± 0.06 in $P2Y_4^{0/-}$ mice (mean ± SEM; $N = 10$;

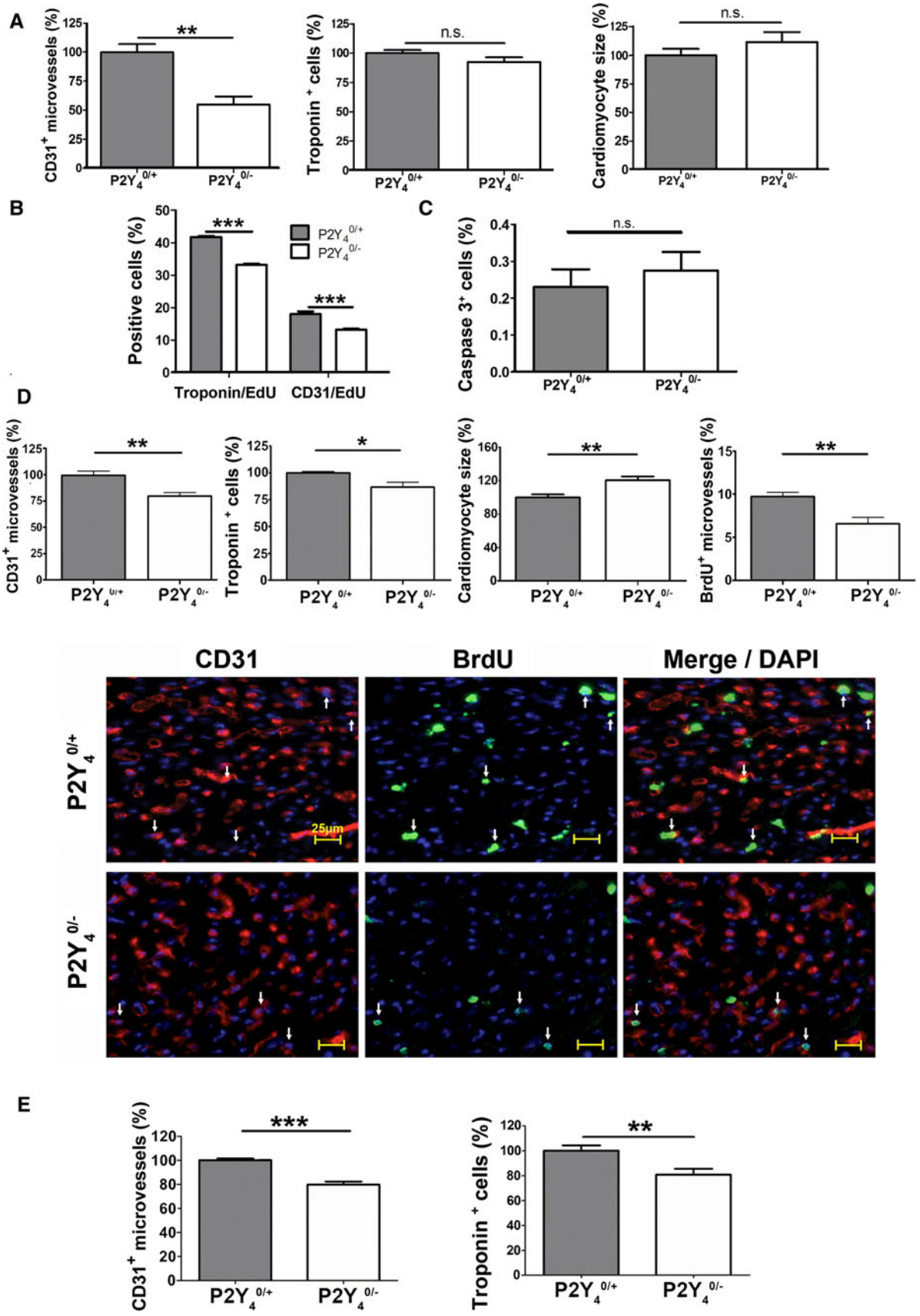
A
CD31+ microvessels (%)
**
Troponin+ cells (%)
n.s.
Cardiomyocyte size (%)
n.s.
P2Y4 0/+
P2Y4 0/-
B
Positive cells (%)
***
***
Troponin/EdU
CD31/EdU
C
Caspase 3+ cells (%)
n.s.
D
CD31+ microvessels (%)
**
Troponin+ cells (%)
*
Cardiomyocyte size (%)
**
BrdU+ microvessels (%)
**
CD31
BrdU
Merge / DAPI
25µm
E
CD31+ microvessels (%)
***
Troponin+ cells (%)
**

◀ **Fig. 3** Microvessel and cardiomyocyte proliferation defect in $P2Y_4$-null mice. **a** Quantification of CD31 and troponin positive cells, and cardiomyocyte size in the hearts of 5 days old $P2Y_4^{0/+}$ and $P2Y_4^{0/-}$ mice. The histological data were blindly obtained at ×20 magnification in 5 fields on transversal sections. Histological and flow cytometry data represent the mean ± SEM of 9 $P2Y_4^{0/+}$ and 9 $P2Y_4^{0/-}$ hearts from 5 days old mice. **b** Quantification of troponin/EdU and CD31/EdU positive cells by flow cytometry in the hearts of 5 days old $P2Y_4^{0/+}$ and $P2Y_4^{0/-}$ mice. The flow cytometry data represent the mean ± SEM of 9 $P2Y_4^{0/+}$ and 9 $P2Y_4^{0/-}$ hearts from 5 days old mice. **c** Quantification of active caspase 3 positive cells in the hearts of 5 days old $P2Y_4^{0/+}$ and $P2Y_4^{0/-}$ mice. The histological data were blindly obtained at ×20 magnification in 5 fields on transversal sections. Histological data represent the mean ± SEM of 5 $P2Y_4^{0/+}$ and 5 $P2Y_4^{0/-}$ hearts from 5 days old mice. **d** Quantification of CD31 and CD31/BrdU positive microvessels, troponin positive cells and cardiomyocyte size in the hearts of 10 days old $P2Y_4^{0/+}$ and $P2Y_4^{0/-}$ mice. The results were blindly counted at ×20 magnification in 15 fields on transversal sections, covering at least 40 % of the heart. Results represent the mean ± SEM of 10 $P2Y_4^{0/+}$ and 10 $P2Y_4^{0/-}$ hearts from 10 days old mice. Immunofluorescent detection of CD31/BrdU positive cells in 10 days old $P2Y_4^{0/+}$ and $P2Y_4^{0/-}$ hearts was performed at ×20 magnification showing co-localization of BrdU (*green*) and CD31 (*red*) in 10 days old $P2Y_4^{0/+}$ and $P2Y_4^{0/-}$ mice. The nucleus is stained by DAPI (*blue*). Arrows indicate examples of microvessels identified by a double BrdU/CD31 labelling. **e** Quantification of CD31 and troponin positive cells in the hearts of adult $P2Y_4^{0/+}$ and $P2Y_4^{0/-}$ mice. CD31 and troponin positive cells were blindly counted at ×20 magnification in 15 fields on transversal sections. The results are the mean ± SEM of 8 $P2Y_4^{0/+}$ and 8 $P2Y_4^{0/-}$ hearts from 12 weeks old mice. (Color figure online)

$^{**}p < 0.01$) corresponding to a reduction of 22 % (Fig. 4b; right panel). The magnitude of these differences was comparable to the effect of dexamethasone (0.5 mg/kg) or blocking antibodies against Flk-1 VEGF receptor in the same model (data not shown).

Discussion

Knockout mice for several target genes have been reported to display heart development defects related to loss of their expression in cardiomyocytes and cardiomyocyte dysfunction. Knockout mice for $\alpha_{1A/C}$ and α_{1B} adrenergic receptors [20], androgen receptor [21] or serotonin 2B receptor [22] display smaller hearts due to smaller cardiomyocytes [20] or reduction of their proliferation [21, 22]. On the other hand, neuropilin-1 or creatine kinase knockout mice display hearts with an enhanced size due to cardiomyocyte hypertrophy [23, 24]. In VEGF-B knockout mice, heart weight was significantly decreased 6 weeks after birth [25]. However no impaired growth of the vascular network was observed in VEGF-B knock-out mice. The authors suggest that the observed microcardia phenotype could be related to an effect of VEGF-B on cardiomyocyte growth [25].

In this paper we report that $P2Y_4$-deficient mice display a defective cardiac post-natal development resulting in a decreased heart weight and a significant reduction in left ventricle mass, as well as in septal and posterior wall thickness, as measured by echocardiography. $P2Y_4$ expression was previously demonstrated in the embryonic cardiovascular system and more precisely in the developing rat heart [4, 6]. RT-PCR and in situ hybridization experiments revealed $P2Y_4$ expression in heart microvessels but not in cardiomyocytes.

Functional assays confirmed that the $P2Y_4$ receptor is expressed in cardiac ECs, but not in cardiomyocytes. Indeed the Ca^{2+} response to UTP measured in cardiomyocytes was maintained in $P2Y_4^{0/-}$ mice, but completely lost in $P2Y_2^{-/-}$ mice. Interestingly the absence of $P2Y_4$ receptor reduced the growth and migratory capacity of cardiac ECs in vitro. ECs secrete mediators modulating cardiomyocyte development such as PDGF-B and neuregulin-1. We observed a $P2Y_4$-mediated UTP effect on PDGF-B expression in cardiac ECs and lower PDGF-B serum levels in $P2Y_4$-deficient mice. PDGF-B is important for murine cardiac development [26] and more generally for the normal structure and function of conduit vessels and capillaries [27]. Endothelial-specific ablation of PDGF-B leads to cardiac disorders including myocardial hypotrophy and septal abnormalities [28]. The direct involvement of PDGF-B defect in the microcardia phenotype of $P2Y_4$-deficient mice is still not demonstrated since no early post-natal disorder was observed.

The dramatic increase in heart weight during the first weeks after birth is believed to result from massive growth of the coronary vessels and capillaries leading to cardiomyocyte proliferation [25, 29]. When cardiomyocyte DNA synthesis is complete, further growth of the heart is due to cardiomyocyte hypertrophy, that is inhibited in $\alpha_{1A/C}$ and α_{1B} double knockout mice, indicating the role of sympathetic innervations [20]. The in vivo proliferation of microvascular ECs and cardiomyocytes was significantly reduced in the hearts of 5 days old $P2Y_4^{0/-}$ mice. The absence of $P2Y_4$ expression in cardiomyocytes supports that the proliferative defect of cardiomyocytes is an indirect consequence of the angiogenic defect leading to a reduced heart weight at adult age. The proliferation defect of microvessels was correlated with a strong decrease in their density in the hearts of 5 days old $P2Y_4$-deficient mice. Interestingly the decrease in cardiomyocyte proliferation was compensated by an increased size observed in 10 days old $P2Y_4$-deficient mice. The cardiac phenotype of $P2Y_4$-deficient mice is thus opposite to that of $p27^{KIP1}$ knockout mice [30] and transgenic mice expressing c-myc constitutively in cardiomyocytes [31], which is characterized by increased heart weight, with enhanced proliferation and decreased size of cardiomyocytes.

Communication between ECs and cardiomyocytes is thus critical not only during early heart development but also for

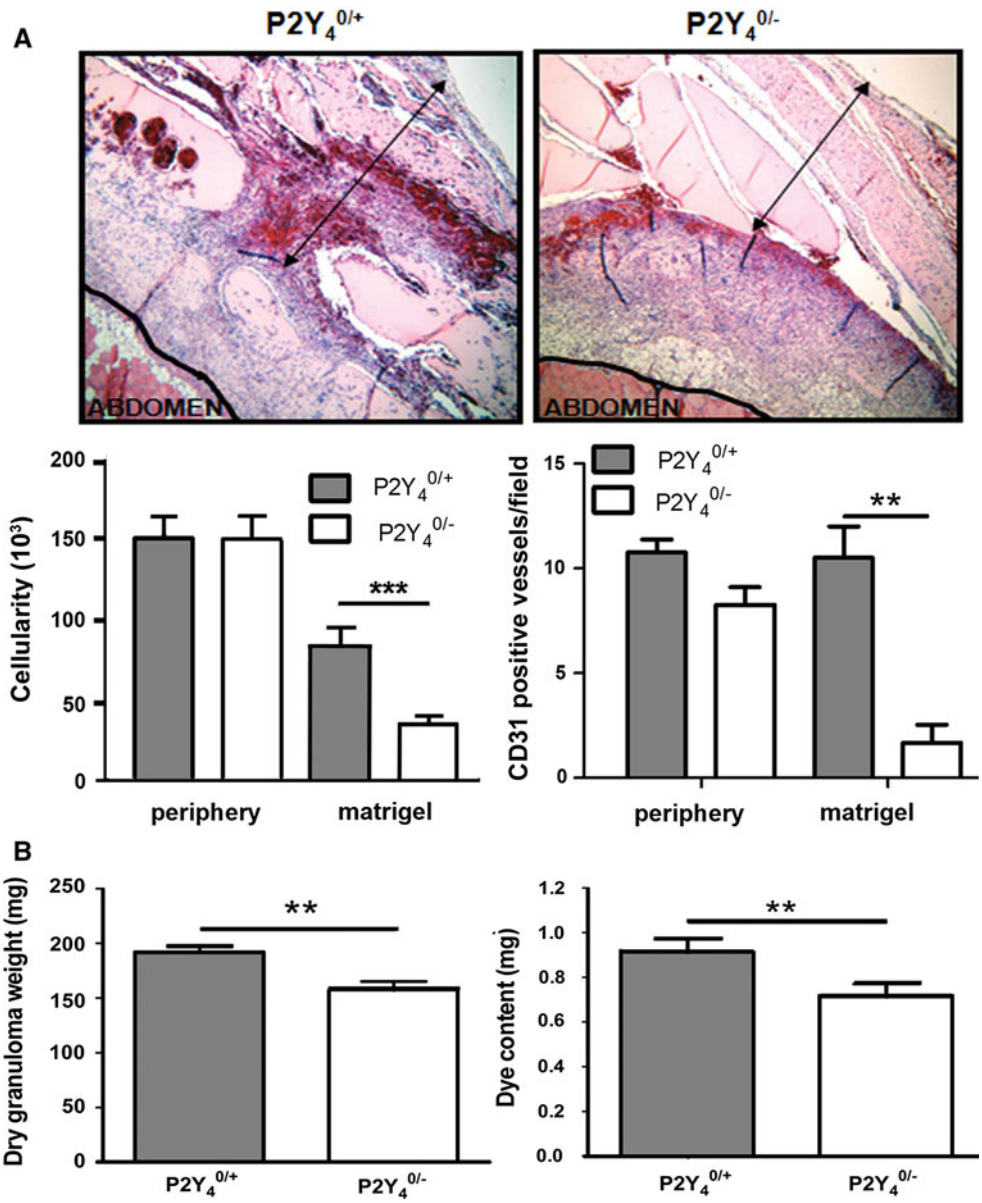

Fig. 4 Cellular infiltration defect in angiogenesis-induced models in $P2Y_4$-null mice. **a** Reduced cellular infiltration in matrigel bulbs injected in $P2Y_4^{0/+}$ and $P2Y_4^{0/-}$ mice. Matrigel was injected in $P2Y_4^{0/+}$ and $P2Y_4^{0/-}$ mice and colored with haematoxylin-eosin after 14 days (×10). Cellularities and CD31 positive cells were counted at day 14 at the periphery and in the matrigel injected in $P2Y_4^{0/+}$ and $P2Y_4^{0/-}$ mice (indicated by the *double arrow*) (N = 6). **b** Air pouch granuloma analysis in $P2Y_4^{0/+}$ and $P2Y_4^{0/-}$ mice. Air pouches were raised on the dorsal surface of 10 $P2Y_4^{0/+}$ and 10 $P2Y_4^{0/-}$ mice under anesthesia. Eight days after angiogenesis induction, intravenous injection of carmine red and gelatin was performed. The granuloma tissue was then removed to determine its dry weight and its carmine content

adult heart function and remodelling [1, 32]. Indeed transgenic expression of the angiogenic factor PR39 in the heart induced ECs proliferation and myocardial hypertrophy [33]. In a similar way, the transgenic induction of an activated Akt1 in the heart led initially to cardiac hypertrophy associated with coronary angiogenesis, whereas angiogenesis was reduced at a later stage leading to heart failure [34].

The potential angiogenic action of extracellular nucleotides was described in ECs present in arteries or vessels. UTP was shown to exert chemotactic and mitogenic actions on guinea pig coronary ECs as well as an angiogenic action on the chorioallantoic membrane [35]. The involvement of $P2Y_2$ and possibly $P2Y_4$ receptors in the chemotactic action of extracellular nucleotides was demonstrated in HUVECs [36]. In pulmonary artery vasa vasorum ECs, extracellular ATP was described as a pro-angiogenic factor [37], and $P2Y_1$- and $P2Y_{13}$-mediated proliferative responses were demonstrated [38]. The angiogenic action of extracellular nucleotides on microvessels was not described so far, and more interestingly in the context of a defective organ development.

The identification of $P2Y_4$ expression in cardiac ECs was an unexpected finding knowing the very restricted tissue distribution of $P2Y_4$ receptor compared to that of ubiquitous $P2Y_1$ and $P2Y_2$ receptors. The remaining effect of UTP on EC proliferation and migration in $P2Y_4$ knockout ECs is likely due to the $P2Y_2$ receptor, which displays a similar pharmacological profile. Unaltered responses to UTP and ATP have been observed in aortic ECs from $P2Y_4$-null mice [39]. It appears thus that while $P2Y_1$ and $P2Y_2$ receptors are mediating nucleotide effects

on aortic ECs, the $P2Y_4$ receptor plays a determinant role in microvascular ECs physiology. We detected $P2Y_4$ expression in human heart and more precisely in human cardiac microvessels. The potential antiangiogenic action of $P2Y_4$ antagonists could have promising therapeutical applications.

Interestingly the angiogenic defect observed in matrigel and air pouch granuloma models in vivo suggests the expression and role of $P2Y_4$ in other microvascular beds as well. Interestingly matrigel invasion was also decreased in ectonucleotidase CD39 knockout mice [40]. One explanation proposed by the authors is that the accumulation of ATP resulting from CD39 deficiency leads to impaired chemotaxis of macrophages due to $P2Y_2$ receptor desensitization. Multiple P2Y receptors seem thus to play complementary roles in angiogenesis.

Uracil nucleotides were shown to protect cardiomyocytes from hypoxic stress [13], and to reduce infarct size and improve heart function after myocardial infarct [14]. These effects may result from multiple effects of UTP on $P2Y_2$ receptors expressed on cardiomyocytes and on endothelial $P2Y_2$ and $P2Y_4$ receptors. More recently the $P2Y_6$ receptor was shown to be involved in overload-induced cardiac fibrosis [3]. Furthermore it was demonstrated that mechanical stretch releases nucleotides from cardiomyocytes through pannexin hemichannels [3]. A release of UTP has also been observed in human heart during myocardial infarction [41]. It appears that three P2Y receptors play determinant roles in cardiac functions: $P2Y_2$ in cardioprotection, $P2Y_6$ in cardiac fibrosis and $P2Y_4$ in cardiac development.

The current study constitutes a major advance in the field of nucleotide receptors and cardiac development. Besides VEGF and other angiogenic factors, UTP appears as an important physiological regulator of cardiac endothelial functions acting through $P2Y_4$ receptor activation. Antagonists of the $P2Y_4$ receptor as well as antibodies directed against this nucleotide receptor could reduce excessive angiogenesis. Besides the determinant role of $P2Y_{12}$ and $P2Y_1$ receptors in platelet physiology, $P2Y_4$ receptor could constitute a therapeutic target to regulate cardiac remodelling and post-ischemic revascularisation. In a broader way, our study demonstrates the role of an endothelial receptor in heart growth in vivo and illustrates the involvement of endothelial-cardiomyocyte interactions in cardiac development.

Acknowledgments We thank Larissa di Pietrantonio, Olivier Vosters, Dominique Fokan, Hrag Esfahani and Steven Droogmans for help and technical assistance. The authors are grateful to Dr Andreas Markl for invaluable assistance in telemetry and helpful discussion. This work was supported by an Action de Recherche Concertée of the Communauté Française de Belgique, an Interuniversity Attraction Pole grant from the Politique Scientifique Fédérale (IAP-P6/30), Prime Minister's Office, Federal Service for Science, Technology and Culture, by grants of the Fonds de la Recherche Scientifique Médicale (F.R.S.M.), the Fonds d'Encouragement à la Recherche (F.E.R.), the Fonds Emile DEFAY, the Fonds de la Recherche Scientifique Médicale of Belgium, the Walloon Region (Programme d'Excellence CIBLES), and the LifeSciHealth programme of the European Community (grant LSHB-2003-503337). D. Communi and C. Dessy are Senior Research Associates of the Fonds National de la Recherche Scientifique (F.N.R.S.). M. Horckmans is supported by the Fonds National de la Recherche Scientifique/FRIA, Belgium. Philippe Unger has received a grant from the "Fonds pour la Chirurgie Cardiaque", Elvira Leon-Gomez is supported by a grant of the F.S.R. (Fonds Spécial de Recherche) of the U.C.L. (Université catholique de Louvain). The funders had no role in study design, data collection and analysis, decision to publish, or preparation of the manuscript.

Conflict of interest None.

References

1. Hsieh PC, Davis ME, Lisowski LK, Lee RT (2006) Endothelial-cardiomyocyte interactions in cardiac development and repair. Annu Rev Physiol 68:51–66
2. Dutta AK, Sabirov RZ, Uramoto H, Okada YR (2004) Role of ATP-conductive anion channel in ATP release from neonatal rat cardiomyocytes in ischaemic or hypoxic conditions. J Physiol 559:799–812
3. Nishida M, Sato Y, Uemura A, Narita Y, Tozaki-Saitoh H, Nakaya M, Ide T, Suzuki K, Inoue K, Nagao T, Kurose H (2008) P2Y6 receptor-Galpha12/13 signalling in cardiomyocytes triggers pressure overload-induced cardiac fibrosis. EMBO J 27(23):3104–3115
4. Cheung KK, Ryten M, Burnstock G (2003) Abundant and dynamic expression of G protein coupled P2Y receptors in mammalian development. Dev Dyn 228:254–266
5. Communi D, Pirotton S, Parmentier M, Boeynaems JM (1995) Cloning and functional expression of a human uridine nucleotide receptor. J Biol Chem 270(52):30849–30852
6. Bogdanov YD, Wildman SS, Clements MP, King BF, Burnstock G (1998) Molecular cloning and characterization of rat P2Y4 nucleotide receptor. Br J Pharmacol 124(3):428–430
7. Webb TE, Henderson D, Roberts JA, Barnard EA (1998) Molecular cloning and characterization of the rat P2Y4 receptor. J Neurochem 71(4):1348–1357
8. Lazarowski ER, Rochelle LG, O'Neal WK, Ribeiro CM, Grubb BR, Zhang V, Harden TK, Boucher RC (2001) Cloning and functional characterization of two murine uridine nucleotide receptors reveal a potential target for correcting ion transport deficiency in cystic fibrosis gallbladder. J Pharmacol Exp Ther 297(1):43–49
9. Lustig KD, Shiau AK, Brake AJ, Julius D (1993) Expression cloning of an ATP receptor from mouse neuroblastoma cells. Proc Natl Acad Sci USA 90(11):5113–5117
10. Robaye B, Ghanem E, Wilkin F, Fokan D, Van Driessche W, Schurmans S, Boeynaems JM, Beauwens R (2003) Loss of nucleotide regulation of epithelial chloride transport in the jejunum of P2Y4-null mice. Mol Pharmacol 63(4):777–783
11. Ghanem E, Robaye B, Leal T, Leipziger J, Van Driessche W, Beauwens R, Boeynaems JM (2005) The role of epithelial P2Y2 and P2Y4 receptors in the regulation of intestinal chloride secretion. Br J Pharmacol 146(3):364–369
12. Matos JE, Sorensen MV, Geyti CS, Robaye B, Boeynaems JM, Leipziger J (2007) Distal colonic Na(+) absorption inhibited by

luminal P2Y(2) receptors. Pflugers Arch Eur J Physiol 454: 977–987
13. Yitzhaki S, Shneyvays V, Jacobson KA, Shainberg A (2005) Involvement of uracil nucleotides in protection of cardiomyocytes from hypoxic stress. Biochem Pharmacol 69:1215–1223
14. Yitzhaki S, Shainberg A, Cheporko Y, Vidne BA, Sagie A, Jacobson KA, Hochhauser E (2006) Uridine-5′-triphosphate (UTP) reduces infarct size and improves rat heart function after myocardial infarct. Biochem Pharmacol 72:949–955
15. Vanderhaeghen P, Lu Q, Prakash N, Frisén J, Walsh CA, Frostig RD, Flanagan JG (2000) A mapping label required for normal scale of body representation in the cortex. Nat Neurosci 3: 358–365
16. Marelli-Berg FM, Peek E, Lidington EA, Stauss HJ, Lechler RI (2000) Isolation of endothelial cells from murine tissue. J Immunol Methods 244:205–215
17. Alvarez BV, Johnson DE, Sowah D, Soliman D, Light PE, Xia Y, Karmazyn M, Casey JR (2007) Carbonic anhydrase inhibition prevents and reverts cardiomyocyte hypertrophy. J Physiol 579(1):127–145
18. Falk W, Goodwin RH, Leonard EJ (1980) A 48-well micro chemotaxis assembly for rapid and accurate measurement of leucocyte migration. J Immunol Methods 33:239–247
19. Colville-Nash PR, Alam CA, Appleton I, Brown JR, Seed MP, Willoughby DA (1995) The pharmacological modulation of angiogenesis in chronic granulomatous inflammation. J Pharmacol Exp Ther 274(3):1463–1472
20. O'Connell TD, Ishizaka S, Nakamura A, Swigart PM, Rodrigo MC, Simpson GL, Cotecchia S, Rokosh DG, Grossman W, Foster E, Simpson PC (2003) The alpha(1A/C)- and alpha(1B)-adrenergic receptors are required for physiological cardiac hypertrophy in the double-knockout mouse. J Clin Invest 111:1783–1791
21. Ikeda Y, Aihara K, Sato T, Akaike M, Yoshizumi M, Suzaki Y, Izawa Y, Fujimura M, Hashizume S, Kato M, Yagi S, Tamaki T, Kawano H, Matsumoto T, Azuma H, Kato S, Matsumoto T (2005) Androgen receptor gene knockout male mice exhibit impaired cardiac growth and exacerbation of angiotensin II-induced cardiac fibrosis. J Biol Chem 280(33):29661–29666
22. Nebigil CG, Choi DS, Dierich A, Hickel P, Le Meur M, Messaddeq N, Launay JM, Maroteaux L (2000) Serotonin 2B receptor is required for heart development. Proc Natl Acad Sci USA 97:9508–9513
23. Nahrendorf M, Spindler M, Hu K, Bauer L, Ritter O, Nordbeck P, Quaschning T, Hiller KH, Wallis J, Ertl G, Bauer WR, Neubauer S (2005) Creatine kinase knockout mice show left ventricular hypertrophy and dilatation, but unaltered remodeling post-myocardial infarction. Cardiovasc Res 65:419–427
24. Ellmers LJ, Knowles JW, Kim HS, Smithies O, Maeda N, Cameron VA (2002) Ventricular expression of natriuretic peptides in $Nrp1^{-/-}$ mice with cardiac hypertrophy and fibrosis. Am J Physiol Heart Circ Physiol 283:707–714
25. Bellomo D, Headrick JP, Silins GU, Paterson CA, Thomas PS, Gartside M, Mould A, Cahill MM, Tonks ID, Grimmond SM, Townson S, Wells C, Little M, Cummings MC, Hayward NK, Kay GF (2000) Mice lacking the vascular endothelial growth factor-B gene (Vegfb) have smaller hearts, dysfunctional coronary vasculature, and impaired recovery from cardiac ischemia. Circ Res 86:e29–e35
26. Van den Akker NM, Winkel LC, Nisancioglu MH, Maas S, Wisse LJ, Armulik A, Poelmann RE, Lie-Venema H, Betsholtz C, Gittenberger-de Groot AC (2008) PDGF-B signaling is important for murine cardiac development: its role in developing atrioventricular valves, coronaries, and cardiac innervation. Dev Dyn 237(2):494–503
27. Nyström HC, Lindblom P, Wickman A, Andersson I, Norlin J, Fäldt J, Lindahl P, Skøtt O, Bjarnegård M, Fitzgerald SM, Caidahl K, Gan LM, Betsholz C, Bergström G (2006) Platelet-derived growth factor B retention is essential for development of normal structure and function of conduit vessels and capillaries. Cardiovasc Res 71(3):557–565
28. Bjarnegård M, Enge M, Norlin J, Gustafsdottir S, Fredriksson S, Abramsson A, Takemoto M, Gustafsson E, Fässler R, Betsholtz C (2004) Endothelium-specific ablation of PDGFB leads to pericyte loss and glomerular, cardiac and placental abnormalities. Development 131(8):1847–1857
29. Hudlicka O, Brown MD (1996) Postnatal growth of the heart and its blood vessels. J Vasc Res 33:266–287
30. Poolman RA, Li JM, Durand B, Brooks G (1999) Altered expression of cell cycle proteins and prolonged duration of cardiac myocyte hyperplasia in p27KIP1 knockout mice. Circ Res 85:117–127
31. Jackson T, Allard MF, Sreenan CM, Doss LK, Bishop SP, Swain JL (1990) The c-myc proto-oncogene regulates cardiac development in transgenic mice. Mol Cell Biol 10:3709–3716
32. Brutsaert DL (2003) Cardiac endothelial-myocardial signaling: its role in cardiac growth, contractile performance, and rhythmicity. Physiol Rev 83:59–115
33. Tirziu D, Chorianopoulos E, Moodie KL, Palac RT, Zhuang ZW, Tjwa M, Roncal C, Eriksson U, Fu Q, Elfenbein A, Hall AE, Carmeliet P, Moons L, Simons M (2007) Myocardial hypertrophy in the absence of external stimuli is induced by angiogenesis in mice. J Clin Invest 117:3188–3197
34. Shiojima I, Sato K, Izumiya Y, Schiekofer S, Ito M, Liao R, Colucci WS, Walsh K (2005) Disruption of coordinated cardiac hypertrophy and angiogenesis contributes to the transition to heart failure. J Clin Invest 115(8):2059–2064
35. Satterwhite CM, Farrelly AM, Bradley ME (1999) Chemotactic, mitogenic, and angiogenic actions of UTP on vascular endothelial cells. Am J Physiol 276:1091–1097
36. Kaczmarek E, Erb L, Koziak K, Jarzyna R, Wink MR, Guckelberger O, Blusztajn JK, Trinkaus-Randall V, Weisman GA, Robson SC (2005) Modulation of endothelial cell migration by extracellular nucleotides. Involvement of focal adhesion kinase and phosphatidylinositol 3-kinase-mediated pathways. Thromb Haemost 93(4):735–742
37. Gerasimovskaya EV, Woodward HN, Tucker DA, Stenmark KR (2008) Extracellular ATP is a pro-angiogenic factor for pulmonary artery vasa vasorum endothelial cells. Angiogenesis 11: 169–182
38. Lyubchenko T, Woodward H, Veo KD, Burns N, Nijmeh H, Liubchenko GA, Stenmark KR, Gerasimovskaya EV (2011) P2Y1 and P2Y13 receptors mediate Ca^{2+} signaling and proliferative responses in pulmonary artery vasa vasorum endothelial cells. Am J Physiol Cell Physiol 300:C266–C275
39. Guns PJ, Korda A, Crauwels HM, Van Assche T, Robaye B, Boeynaems JM, Bult H (2005) Pharmacological characterization of nucleotide P2Y receptors on endothelial cells of the mouse aorta. Br J Pharmacol 146(2):288–295
40. Goepfert C, Sundberg C, Sevigny J, Enjyoji K, Hoshi T, Csizmadia E, Robson E (2001) Disordered cellular migration and angiogenesis in cd39-null mice. Circulation 104(25):3109–3115
41. Wihlborg AK, Balogh J, Wang L, Borna C, Dou Y, Joshi BV, Lazarowski E, Jacobson KA, Arner A, Erlinge D (2006) Positive inotropic effects by uridine triphosphate (UTP) and uridine diphosphate (UDP) via P2Y2 and P2Y6 receptors on cardiomyocytes and release of UTP in man during myocardial infarction. Circ Res 98:970–976